## ARTIFICIAL HEARTS AND OTHER ORGANS

Organ transplantation from suitable donors is a medical technology posing risks of tissue rejection which are well-handled today by suitable drug regimen. Widespread application of this technology is severely limited by the shortage of suitable donor organs. Artificial organ systems, constructed of human-made materials, are generally not subject to rejection problems, nor is organ availability of prime concern. However, their development and use poses its own set of challenges.

The heart, liver, kidney, and other organs perform functions which are not fully understood by modern science. Artificial organs for implant therefore provide at best an incomplete solution to a medical problem, but a solution which can be satisfactory in some cases. Such intervention generally involves the implantation of nonbiological elements within the body, raising issues of biocompatability, and requiring stringent sterilization protocols. The use of implanted human-made structures, such as heart valves in contact with circulating blood, has been associated with an increased incidence of thromboembolic events.

This article considers the energy requirements, and the sensor and control aspects of the design of artificial hearts and of systems designed to augment the cardiovascular pumping provided by a failing heart. Sensor, control, and energy requirements are common to other organs as well, and these requirements will be discussed in relation to the artificial pancreas and other artificial organs.

### ENERGETICS OF BLOOD PUMPING

The heart does a substantial amount of work in pumping blood through the body. Pumping a mean flow, or cardiac output (CO), of 5 L/min to an aortic pressure head of 13.3 kPa (100 mm Hg) requires a work rate of 1.1 W. The most energy-dense batteries available, lithium primary cells, have a capacity less than 500 Wh/kg. Nearly 20 kg of batteries would be required to store the energy for one year of operation under the very best of conditions.

In fact, neither the natural heart nor the human-made pumps designed to replace it are particularly energy efficient. Obtainable efficiencies vary with CO, ranging from about 10 to about 25% for natural and human-made analogs. Therefore, a substantial energy source must be provided for blood pumping. Transcutaneous energy transmission using magnetic induction coupling is one means of powering an implanted pump and is the preferred system for proposed human-made blood pump implants. The energy derived from metabolism of food is another, and is the source of energy for proposed muscle-powered blood pumps.

### CONTROL OF CARDIOVASCULAR PRESSURE AND FLOW

The mammalian cardiovascular (CV) system has evolved elaborate and redundant systems for dealing with shifts in physiological need. When demand for gas exchange increases, the CO may increase from 5 to 15 L/min in response. The force of contraction is related to the degree of ventricular filling (preload) through the Frank–Starling mechanism. In addition both the force of contraction and the heart rate are modified appropriately by the rapid response of the autonomic nervous system, and by a slower but longer acting endocrine response. In a healthy CV system, this CO increase is carried out while maintaining the blood pressure within a narrow range. For this to occur, the CO and the hydraulic impedance of the cardiovascular system change in opposite directions.

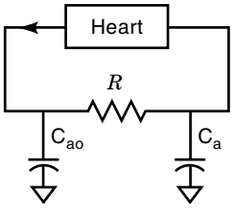


**Figure 1.** Heart pumping into a 3-element lumped-parameter circulation model representing aortic $C_{ao}$ and atrial $C_a$ compliances and systemic resistance $R$.

Consider the simplified one-sided lumped-parameter CV system consisting of aortic and venous compliances and a systemic resistance in Fig. 1. The venous compliance includes the right atrium, and has been labeled $C_a$. The pulmonary circulation is included as part of the heart pump in this representation.

The circulating blood volume (BV) consists of that within the aortic compliance ($P_{ao}C_{ao}$) plus that within the venous compliance ($P_aC_a$) plus the mean volume in the heart, BH. The following relations apply, where all quantities are to be interpreted as their mean values:

$$\mathrm{BV} = \mathrm{BH} + P_{ao}C_{ao} + P_aC_a \tag{1}$$

$$P_{ao} - P_a = \mathrm{CO} \times R \tag{2}$$

Equations (1) and (2) combine to yield:

$$P_{ao} + 1/C_a(\mathrm{BH} - \mathrm{BV}) = (C_a/(C_{ao} + C_a))(\mathrm{CO} \times R) \tag{3}$$

The natural cardiovascular control system employs a distributed network of baro- and chemoreceptors to respond to increased oxygen need by increasing heart rate and cardiac contractility which may increase CO by a factor of three within a few seconds. There is a need to maintain $P_{ao}$ within narrow limits, and blood volumes do not change rapidly. The CV control system responds to CO increases by decreasing both $R$ and $C_a$ so as to keep $P_{ao}$ at a safe level as shown in Eq. (3). Mechanical systems meant to augment or replace the heart are faced with the dual challenges of responding to changes in flow requirements and providing a means for pressure to remain within safe limits despite these flow changes.

## APPROACHES TO MECHANICAL DESIGN OF ARTIFICIAL HEARTS

Circulatory support devices encompass a wide variety of pump designs, which reflect various approaches to the method of actuation, anatomical placement, and desired blood flow patterns within the pumping chamber. Devices may be generally categorized as either positive displacement or continuous flow.

Positive displacement pumps produce pulsatile flow in similar fashion to the natural heart, with alternate filling and ejection phases. Inlet and outlet valves maintain unidirectional blood flow. A variety of actuation methods and pump chamber designs have been developed (Table 1). Early designs using large pneumatic drivers to provide alternating pressure and vacuum pulses to a drive line (flexible tubing) attached to the pump housing are in common use, but patient mobility is limited. Brushless dc motors (BDCM) or solenoid actuators coupled directly to the pumping chamber allow patients sufficient mobility to return to normal activities. In the newer systems currently under development (1–4), power is inductively transferred to an implanted controller, thereby eliminating the risk of infection associated with percutaneous cable sites.

Continuous flow pumps use high-speed rotating impellers in the blood stream to produce axial or centrifugal flow without the need for valves. These pumps have the potential to be significantly smaller than positive displacement pumps. Developers of systems intended for long-term implantation include: Nimbus (Rancho Cordova, CA) and the University of Pittsburgh (5); Transicoil, Inc. (Valley Forge, PA) and the Texas Heart Institute (Houston) (6); the Cleveland Clinic Foundation and the University of Utah (7); Baylor College of Medicine and NASA/Johnson Space Center (Houston) (8). Current research focuses on reducing fluid stresses on the blood, developing durable and antithrombogenic bearings, and refining control methods.

One design approaching in vivo durability testing in total artificial heart (TAH) and ventricular assist device (VAD) configurations is the rollerscrew/pusherplate system developed by Penn State/3M Healthcare/Arrow International and about which we will focus our examples of calculations. Placement of motor, electronics/battery cannister, transcutaneous transmitter, and an external case for carrying batteries is illustrated in Fig. 2 for the TAH System.

## SIMULATION OF PUMP PERFORMANCE AND TAH CONTROL

Human-made blood pumps are often performance-tested using a mock circulatory loop, a group of mechanical elements which simulate the hydraulic impedance of the cardio-vascular system. An alternate approach is the use of computer simulation. This approach has the advantage of allowing hydraulic compliance and resistance elements to change rapidly to values which reflect cardiovascular control response. We show here some examples of such calculations. The narrative in the section on TAH control was copyrighted in 1995 by IEEE. Reprinted, with permission, from proceedings of the NE Bioengineering Conference, Bar Harbor, ME, May, 1995, pp. 22–23.

Physically, the TAH we consider consists of a small brushless dc motor driving an efficient rotary to linear conversion mechanism. The resulting motion drives a circular pusherplate which compresses a flexible ventricle against a rigid case. Pusherplates are attached to both sides of the motor drive, so that blood is ejected from one ventricle as the other is passively filling.

The controller of this TAH has three main tasks: controlling the applied motor voltage on a stroke to stroke basis so that the pusherplate follows a desired trajectory, maintaining balance between the systemic and pulmonary circulations by manipulating the relative filling periods of the left and right ventricles, and varying overall cardiac output in response to demand (9,10). Studies have shown that, due to elevated venous pressures, an output control method based on the Star-

**Table 1. Circulatory Support Systems Utilizing Positive Displacement Pumps Currently under Advanced Development for Bridge-to-Transplant and/or Long-Term Use**

| Developer | Type | Force Transducer | Coupling to Blood Pump |
|---|---|---|---|
| Thermo Cardiosystems (Woburn, MA) | VAD | Low-speed unidirectional BDCM | Helical cam → pusherplate → diaphragm |
| Thermo Cardiosystems (Woburn, MA) | VAD | External pneumatic driver | Drive line → pusherplate → diaphragm |
| Thoratec Laboratories Corp. (Berkeley, CA) | VAD | External pneumatic driver | Drive line → diaphragm → blood sac |
| Novacor Division, Baxter Healthcare (Oakland, CA) | VAD | Pivoting solenoid | Spring arms → dual symmetric pusherplates compressing blood sac |
| CardioWest Technologies (Tucson, AZ) | TAH | External pneumatic driver | Drive line → diaphragm |
| Penn State University (Hershey and University Park, PA); 3M Health-Care (Ann Arbor, MI); Arrow International (Reading, PA) | TAH and VAD | Moderate-speed bidirectional BDCM | Rollerscrew → pusher plate(s) → blood sac(s) |
| Abiomed (Danvers, MA); Texas Heart Institute (Houston, TX) | TAH | High-speed unidirectional BDCM | Axial flow pump → hydraulic fluid → spool valve → blood sacs |
| Nimbus (Rancho Cordova, CA); Cleveland Clinic (Cleveland, OH) | TAH | High-speed unidirectional BDCM | Gear pump → hydraulic fluid → magnetically coupled pusherplates → diaphragms |

Note: The first four systems have achieved a significant level of clinical use.

ling mechanism is insufficient for TAH recipients (10). Therefore, demand is sensed through changes in the systemic arterial pressure. Adjustments are made at intervals of one or more cardiac cycles, with the adjustment of pusherplate velocity (inner loop control) applied more frequently than left–right balance (preload) or demand–response (afterload) control.

Direct measurements of pressures in the TAH and the circulatory system would require additional sensors and transducers, increasing the risk of device failure. It is therefore desirable to estimate these values from the applied voltage and current waveforms of the motor. This requires an accurate representation of motor parameters, and a reasonable representation for the CV system so that time-varying parameters can be inferred, and motor control adjusted.

## TAH Model

A representation for the CV system driven by a TAH is shown in Fig. 3. Key pressures are aortic pressure ($P_{ao}$), pulmonary arterial pressure ($P_{pa}$), left and right atrial pressures ($P_{la}$, $P_{ra}$), and left and right ventricular pressures ($P_{lv}$, $P_{rv}$). The fluid-storing properties of the blood vessels are represented by capacitances (compliances), and resistances $R_{pulm}$ and $R_{sys}$ represent the pressure drop across the pulmonary and systemic capillaries. For the purposes of this model, valves are assumed to open and close instantaneously on pressure differentials. The pressure drop across an open outlet valve is represented by 3 elements in Fig. 3:

$$\Delta P = R_{ov1}Q + R_{ov2}Q^2 + L_{out}\frac{dQ}{dt} \tag{4}$$

where $Q$ is the flow across the valve, $R_{ov1}$ and $R_{ov2}$ are resistance terms, and $L$ is the inertance of the fluid in the outlet graft. The pressure gradient across an open inlet valve, as well as for steady backflow across a closed valve is described as a square law relationship:

$$\Delta P = RQ^2 \tag{5}$$

Here, $R$ varies according to whether the valve is open or closed, as well as with the diameter of the valve, which is different in the inlet and outlet positions.

The ventricles are modeled as pressure-dependent compliances $C_{lv}(P_{lv})$ and $C_{rv}(P_{rv})$, with values determined heuristically in static tests. These tests demonstrate that as the pressure in the ventricle increases, the compliance decreases rapidly, as the flexible blood sac is compressed against the rigid case of the ventricle. The pusherplates act as a flow source (area × velocity) when coupled to the blood sacs, driving blood through the outlet ports. This analysis results in 80 sets of 12 differential equations, with the appropriate set selected depending on the position of the valves and the direction of pusherplate motion. The equations are readily solved by computer using a Runge–Kutta integration method. Pressure and flow waveforms from such a model compare quite favorably with measurements taken from mock circulatory loop tests (11–14).

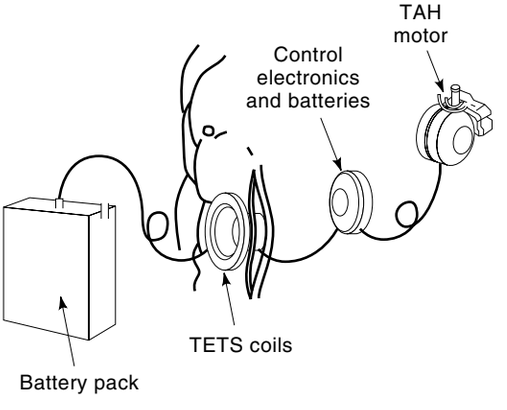


**Figure 2.** Elements of an implanted TAH system include an implanted blood pump, a means of transcutaneous energy transmission using magnetic induction, and an external battery.

## TAH Control Simulation

The velocity profile of the pusherplate is regulated by an adaptive feedforward control mechanism, where the applied

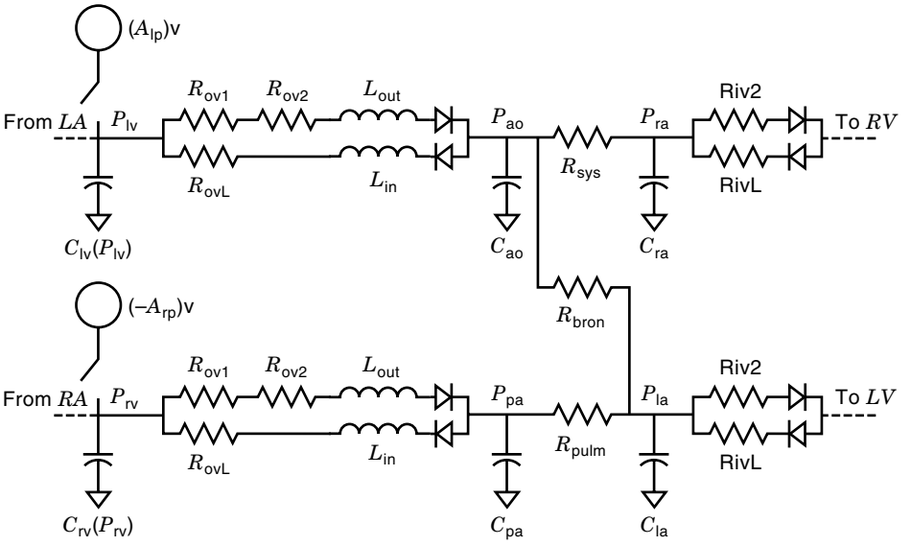


**Figure 3.** Analog of the TAH coupled to the circulatory system. (From Ref. 15, courtesy of IEEE © 1995 by IEEE. All rights reserved.)

motor voltage scheduled for the next stroke cycle is adjusted by a factor proportional to the difference between the desired and actual pusherplate velocities during the previous cycle. Control is scheduled at constant position intervals, corresponding to the commutations of the dc motor, rather than at fixed times.

An estimate of the left ventricular pressure is obtained as follows. For a dc motor, the voltage applied to the motor is

$$e_m = Ri + \frac{K_b}{K_c} v \tag{6}$$

where $R$ is the winding resistance, $i$ is the winding current, $K_b$ is the motor's back emf constant, and $K_c$ is a constant relating the angular velocity of the motor with the linear velocity $v$ of the pusherplate. The motor's torque is related to the current by

$$T = K_t i \tag{7}$$

where $K_t$ is the motor's torque constant. An estimate of the ventricular pressure is formulated by breaking the motor torque into frictional, speed, and load-dependent components, and assuming the force exerted by the load is equal to the pressure inside the ventricle multiplied by the area of the pusherplate. Solving for ventricular pressure yields

$$P_{v(est)} = \frac{1}{K_c A_{lp}} \left( \frac{K_t}{R} \left( e_m - \frac{K_b}{K_c} v \right) - \frac{D}{K_c} v - \frac{J}{K_c} \frac{dv}{dt} - T_f \right) \tag{8}$$

where $A_{lp}$ is the area of the pusherplate, $D$ is a damping coefficient, $J$ is the rotary inertia of the moving parts of the motor, and $T_f$ is a constant frictional torque. Equation (8) forms the basis of the output and balance control methods of the TAH (9,10,15,16). An example of the model's computed ventricular pressure signal is shown in the upper panel of Fig. 4. The lower panel shows the degradation in this signal caused by the limited sampling of position provided by the motor position sensors.

As shown in Fig. 4, when the ventricle fills incompletely, the pusherplate attains considerable forward velocity before coming in contact with the ventricle. This event causes a large initial peak in the ventricular pressure, which damps out quickly. The pressure estimation deviates from that obtained from the model due to the limited rate of the asynchronous position sampling and the inaccuracies this introduces in velocity and acceleration estimation. Nevertheless, the initial pressure peak indicating contact with the pusherplate and blood sac is well represented. The control algorithm ad-

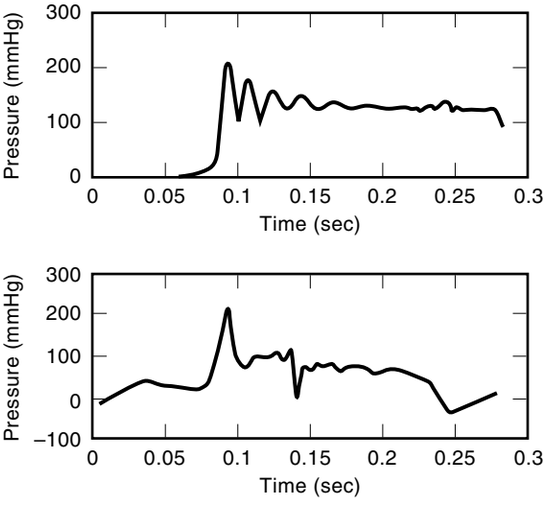


**Figure 4.** Systolic left ventricular pressure from TAH model (top) and estimation of degradation in pressure signal caused by limited sampling of position (bottom). (From Ref. 15, courtesy of IEEE © 1995 by IEEE. All rights reserved.)

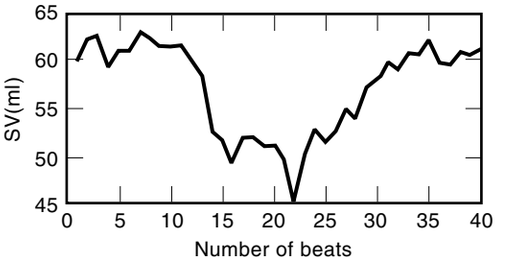


**Figure 5.** Plot of stroke volume (SV) versus time. The pulmonary peripheral resistance is increased at beat 10. (From Ref. 15, courtesy of IEEE © 1995 by IEEE. All rights reserved.)

justs the filling times as needed. If there is incomplete left ventricular filling, the filling times are altered to restore balance. In order to suppress the cardiac output's dependence on right atrial pressure, the left pump filling time is increased when the right pump filling time is decreased, and vice versa. This balance control is implemented every five beats to allow averaging of these fill-rate indicating signals.

This balance control adjustment requires a finite amount of time to implement. This can be shown in the model by allowing a step change in an element ($R_{\text{pulm}}$) of the model. The increase in resistance causes a subsequent reduction in left atrial pressure, which decreases ventricular filling, causing a left–right ventricular imbalance. Figure 5 shows a plot of left ventricular stroke volume versus the number of pump cycles when pulmonary resistance was doubled at beat 10. The decrease in filling pressure causes a steep reduction in the stroke volume. By increasing the left filling time while decreasing the right ventricular rate of filling, the balance control mechanism alone can correct the imbalance. At beat one, the left diastolic time is 0.36 s, but by beat 40 it has been increased to 0.44 s.

There are many aspects of this model of TAH and cardiovascular interaction that need exploration including the dynamics of interaction between autonomic blood pressure regulation and the TAH system's candidate control algorithms.

## VENTRICULAR ASSIST

It is a relatively simple matter to apply the control techniques designed for the TAH to a ventricular assist device (VAD), which accepts blood from the left ventricular apex and returns it to the aorta. The assist device developed by the authors makes use of the same electric motor and force transducer used for the TAH, but has only a single pump and a single pusherplate on the electromechanical drive. Such devices are useful in the large population of patients whose ventricular failure is concentrated in the left ventricle.

The control system for the ventricular assist device, like that for the TAH, must control the pusherplate motion trajectory (inner loop control) and the pump output (outer loop control). The inner loop control algorithm can be implemented as a feed-forward controller as with the TAH. The desired speed trajectories are somewhat different, since the device is exposed to different pressures. In systole, differences occur only due to the additional outflow tract resistance and inertance presented by the outlet cannula that takes blood from the abdominally placed pump to the thoracic aorta. In VAD diastole, the motor is loaded only by the friction and inertia of the mechanism, and so the desired motion trajectory, particularly when energy efficiency is considered, may be substantially different from that used when a pulmonary load is expected.

The outer loop control for the VAD is a subset of the set of algorithms used for the TAH. The primary goal of the VAD output control is to maintain a low pressure in the native ventricle. In doing so, the VAD (1) by definition, accepts all of the output provided by the right heart, and thereby prevents elevated pulmonary pressures, and (2) maintains low pulmonary venous pressures so that the right heart, which is typically afterload-sensitive, can provide as much cardiac output as possible.

Outer loop control of the VAD is accomplished by monitoring left pump filling via Eq. (8), while making incremental increases and decreases in the pump rate. A decrease in pump filling results in an incremental decrease in the pump rate, with the expectation that filling of the pump will be restored. With the pump filling adequately, trial increases in rate are made in order to determine whether a higher pump output can be supported.

## ENERGY UTILIZATION

Kinetic energy imparted by the blood pump to the blood is delivered through a transduction chain that includes the inductive energy transmission system, the power electronics, mechanical force transducer, and finally the blood pump itself. The energy dissipated in each of these elements differs with load condition. Additional energy needed to run the control electronics and maintain charge on the implanted battery must also be provided through the inductive link. This energy expenditure is largely independent of load conditions. Data were measured for a 100 mL TAH operating on a mechanical CV system analog at 10 L/min flow rate into 14.6 kPA (110 mm Hg) pressure head (17). Of a 19.1 W energy expenditure, transcutaneous energy transmission (TETS) accounted for 25%, control electronics for 3%, the motor and its electromechanical linkage and blood pump for 67%, and kinetic energy imparted to the blood for 15%.

Of particular importance to the patient is energy utilization by the implant (as distinct from the TETS), since this determines the run time provided by an implanted battery of a given technology and size, and therefore has a great impact on safety and lifestyle. Energy lost in the various components of the energy chain can be estimated given a model of each component's losses. In accord with standard models and manufacturers' data, we characterize the major components as follows: The electric motor and power semiconductors are described by a resistance, torque constant, constant frictional loss, and speed-dependent frictional loss, the frictional losses occurring due to nonidealities in the magnetic materials. Ball bearings are characterized by constant and speed-dependent friction terms, in accord with the standard model. The rollerscrew mechanism is characterized by an efficiency (force-dependent friction), in accord with data supplied by its manufacturer. We must recognize also that energy is dissipated in accelerating the moving parts of the system, some of which is not recovered when they decelerate at the end of each motion.

Losses in each component were estimated by assuming perfect tracking of the desired motion trajectory, and using a constant pressure to represent the circulatory load. Figure 6 shows model results for a 225 ms blood pump ejection into a mean pressure of 13.3 kPa (100 mm Hg). Torque to overcome each mechanical loss must be provided by the dc motor, and some additional resistive losses in the motor windings occur due to each of these. In this version of the model, these resistive losses are counted as part of the loss in each component. Fortunately, the largest amount of power goes to providing pressure and flow in the pump, although the sum of the losses equals the output power. No single motor component stands out as responsible for the majority of energy loss.

## TRANSCUTANEOUS ENERGY TRANSMISSION AND BATTERIES

Currently available ventricular assist devices have successfully provided circulatory support in patients awaiting cardiac transplantation, for periods exceeding one year (18). However, these devices have all required infection-prone percutaneous access sites for the cables or tubes which power and control the pumps. Transcutaneous energy transmission systems have been under development for many years. Eventual clinical use of completely implanted systems depends not only on the development of these energy transmission systems, but more importantly on attaining the high degree of reliability in all of the implanted components necessary for long-term clinical use.

In a typical application, inductive coupling between implanted and external coils transfers electrical energy across the intact skin, to power the electromechanical pumping device and control electronics, and to provide recharging power for the implanted batteries. Implanted rechargeable batteries provide backup power in the event that the external energy transmission coil is removed, and to allow the patient a brief period of tether-free operation for bathing. A wireless telemetry link may be provided by a separate coil or pair of coils located within the electronics enclosure, infrared sensors placed subcutaneously, or by modulation of the energy transmission system carrier.

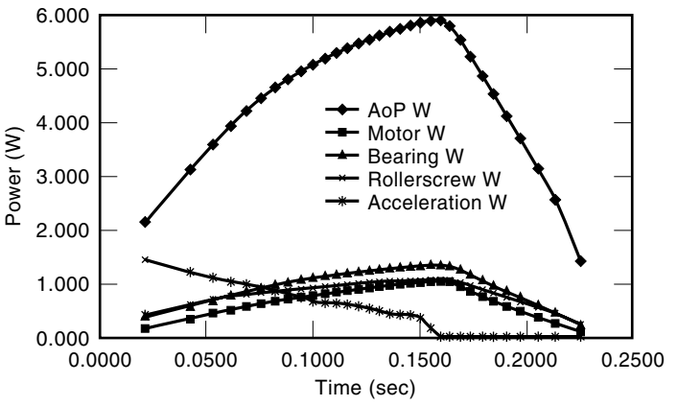


**Figure 6.** Example of model calculations of losses in the energy converter power chain. Results are for a 225 ms systolic ejection into a constant 100 mm Hg load. Losses attributed to each component include $I^2R$ losses in the motor due to the component.

### System Requirements

The design requirements for the energy transmission system, like any power supply design, include input voltage range, output voltage and regulation, output current range, and bandwidth. The input voltage is constrained by the need for a portable, battery power source, most commonly 12 V to 15 V. The output voltage is typically chosen to be higher than the implanted battery voltage and circuit supply voltages, to permit the use of simple recharging and voltage regulation circuits. Typically, an output voltage of 10 V to 15 V is required. Increasing the number of cells to achieve higher voltages results in reduced battery reliability and reduced volumetric efficiency. The design of the control circuit and battery charger usually dictate the voltage regulation requirement (Fig. 7). The output current and bandwidth vary widely, depending on the characteristics of the energy converter and the amount of energy storage provided by capacitors. While most devices require approximately 10 W mean power delivered to the implant, the dynamic power may range from 1 to 70 W during the cardiac cycle.

### Coil Design

The inductive coupling of two coils can be described by the mutual inductance $M$. Mutual inductance can be calculated for two single turn circular axisymmetric coils using Neumann's formula (19). Numerical and closed form methods for the case of angular and lateral displacements are also available (19,20). Multiturn coils are typically considered as a single coil of an estimated mean radius. Empirical coil design formulae (21) or separate Neumann solutions are also used. A useful definition of mutual inductance is

$$M = k\sqrt{L_1 L_2}$$

where $k$ is the coupling coefficient, $L_1$ is the primary coil self inductance, and $L_2$ is the secondary coil self inductance. The coupling coefficient $k$ is a measure of the degree of magnetic flux linkage between the coils, and ranges from zero to one. A high value of $M$ is desirable for attaining high efficiency in power transmission applications, as it represents the best utilization of coil current. The coupling coefficient is increased by reducing the distance between the primary and secondary coil windings, or by directing the flux linkage path through the use of magnetically permeable materials, such as ferrite.

Coupling variation is expected to be common in patients due to lateral, axial, and angular displacements of the primary coil. Consequently, efficiency is reduced and the electrical transfer functions of the link are affected. The significance of transfer function variation depends upon the tolerance of a given system to changes in output (ie, at the implant) voltage and current. In most designs, greater coupling coefficients are obtained at the expense of displacement tolerance. Coil shapes which place the primary windings close to the secondary windings are inherently sensitive to misalignment.

Important factors in coil design are the ease of maintaining alignment, patient comfort and aesthetics, minimization of skin irritation caused by compression or abrasion, and rejection of heat from the coil windings. The secondary coil is usually intended to be implanted subcutaneously, at a depth of 5 mm to 15 mm. An additional problem is the presence of metal (automobile body, appliance, etc.) near the coils,

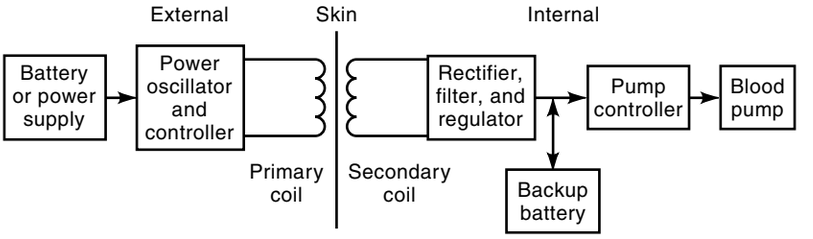


**Figure 7.** Simplified diagram of typical electrical power flow to implanted pump.

which may introduce eddy current and hysteresis losses, and a shift in the coil inductances and mutual inductance (22). In this case, both coil design and drive circuit topology are important.

Equidiameter planar coils achieve high coupling coefficients but are difficult to align without requiring skin pressure. A conical secondary coil and mating primary coil result in improved alignment. For circular coils of differing diameter, a degree of lateral displacement tolerance is achieved when the smaller coil remains within the circumference of the larger coil. If the inner coil is the smaller of the two, and is shaped as a raised mound, then a natural alignment is provided for the loop-shaped primary coil (23,24). Single turn primary and secondary coils encircling the abdomen have also been developed (25).

### Coil Network

The presence of body tissue between and near the coils is of concern, both for operation of the electrical system, and for concern over the possible effects of the electromagnetic fields on the tissue. For frequencies below approximately 500 kHz, power absorption in body tissue due to currents induced by the magnetic field has been shown to be relatively minor, as has dissipation due to dielectric losses (26). Electrical modeling of the coil network and functional testing rarely require inclusion of tissue properties.

Both primary and secondary coils are usually connected to capacitors in either series or in parallel to form resonant circuits in order to reduce the voltage or current levels at the input and output. Commonly, the primary and secondary coil networks are tuned to the same frequency. Operation at resonance causes cancellation of the reactances, which presents a resistive load to the driving circuit. A bipolar switching voltage drive, such as a Class D driver, is used to provide the driving voltage. Operating frequencies range from 100 kHz to 500 kHz. The transcutaneous coil pair and power switching circuits are sources of electromagnetic interference (EMI). Resonant topologies and standard techniques of EMI suppression are necessary to meet regulatory requirements.

The primary and secondary networks may also be tuned to different frequencies. This may be used to compensate coupling-dependent gain variation or to increase the link bandwidth for telemetry (27). In high-power systems, stagger tuning has been applied as a means to maintain both primary and secondary resonance over changing load and coupling conditions (28).

The definition of *gain* for a given system depends on the coil network. For example, the doubly series tuned network can be described as a voltage input, current output network whose gain is the transfer admittance ($I_{out}/V_{in}$). The goals of both a maximum transfer admittance and a minimum coupling-dependent gain variation can be achieved by designing the network to operate at *critical coupling,* which is defined as the condition at which the primary circuit impedance matches the secondary impedance. However, critical coupling does not guarantee maximum efficiency when including input and output voltage constraints.

## CARDIOMYOPLASTY FUNDAMENTALS AND MUSCLE-POWERED BLOOD PUMP

Dynamic cardiomyoplasty (CMP) is a surgical therapy for heart failure which involves the direct application of electrostimulated skeletal muscle for circulatory support. In this procedure, the latissimus dorsi (LD) muscle is isolated, wrapped around the heart, and electrically stimulated to contract during cardiac systole. The potential advantage of this approach is that long-term cardiac assist may be achieved with minimal hardware and low maintenance relative to conventional assist techniques (i.e., mechanical blood pumps). However, questions concerning the mechanism of CMP assist and the long-term efficacy of this approach remain to be answered.

The use of electrically stimulated skeletal muscle as an endogenous power source offers an attractive alternative to the chronic drive systems currently in use. Muscle-powered devices have the potential to greatly simplify cardiac implants by eliminating electromechanical components and avoiding the need to transmit energy across the skin. This approach is especially appealing when one considers the substantial quality-of-life benefits to be derived from a self-contained system free from external components and daily maintenance. Moreover, the relative simplicity of such systems could drastically reduce the cost of long-term cardiac support, increasing its viability from a societal perspective.

The feasibility of biomechanical circulatory support ultimately hinges on the ability of skeletal muscle to generate useful hemodynamic work on a continual basis. The persistent problem of muscle fatigue seemed to preclude such bioactuated systems until 1976 when Salmons and Sreter demonstrated that skeletal muscle could be electrically "conditioned" to resist fatigue (29). Since that time, a number of investigators have quantified the chronic power output of trained skeletal muscle, both in theory and via experimentation (30–33). Predictions of steady-state work capacity range from 2.0 to 15.0 mW/g of muscle tissue. Adopting the lowest figure, one can calculate that a trained muscle weighing 550 g could supply the 1.1 W required to move 5 L of blood each minute across a pressure gradient of 13.3 kPa. This

muscle mass requirement is compatible with the use of human latissimus dorsi (LD) muscle which averages 600 g in the male. However, actual power requirements will depend on the degree of circulatory support needed and the efficiency of muscle power conversion and transmission.

The key to utilizing muscle power for circulatory support lies with the development of a practical scheme by which contractile energy may be collected and efficiently delivered to the bloodstream. The most popular techniques employed to date include wrapping the heart for direct mechanical assistance (cardiomyoplasty), wrapping the aorta for counterpulsation (aortomyoplasty), shaping the muscle into a neoventricle to compress a hydraulic pouch, and positioning a compressive device beneath the muscle midline. However, low power production has proven to be a major disadvantage common to all these assist schemes (34).

The principal cause of this poor performance is the inherent mechanical inefficiency that results when muscle is wrapped to compress the heart or some fluid-filled conduit. Skeletal muscles contain myofibers arranged linearly to produce shortening in one direction. Therefore, muscles arranged in this manner tend to pull and twist the wrapped vessel while providing little force for centralized compression. Likewise, devices placed beneath the muscle midline access only a small fraction of the available energy because their movement is nearly perpendicular to the primary force vector of the muscle.

Another important factor which limits these heterotopic methods is the functional loss brought about via muscle mobilization. Wrap-around techniques require that the muscle be isolated from all surrounding structures, sacrificing collateral blood supply and removing the muscle from its optimal orientation and stretch. The surgical isolation of skeletal muscle has been shown to produce an immediate 37% decrease in contractile power due to trauma and physical separation from surrounding synergistic musculature (35). In the chronic setting, reduced blood flow caused by the separation of collateral blood vessels further compromises function and often leads to ischemia and muscular atrophy (36).

Efforts to optimize the function of wrapped muscle include the use of dynamic training techniques wherein muscles are allowed to shorten (i.e., perform work) during the conditioning process. There is evidence to suggest that skeletal muscles trained in this manner exhibit improved contractile speed and power (37). Work to use such dynamically trained muscles for cardiac support is ongoing and includes the recent development of an axisymmetric blood pump actuated via compression of a fluid-filled elastomeric bladder (38). In this scheme, LD muscle is wrapped around the bladder and stimulated to drive fluid into the pump's housing. There, the fluid compresses a blood-filled, valved conduit and pushes blood from the left ventricle into the aorta.

Given the tensile nature of skeletal muscle contraction, the most effective way to harness muscular work is to employ a linear geometry with the muscle tendon detached from its original insertion and reconnected to a hydraulic energy transmission device. Such an arrangement offers a three-fold advantage in that natural contractile mechanics are preserved, blood flow to the muscle is maintained, and power transfer efficiency is optimized.

Early attempts to harvest in situ skeletal muscle for cardiac assist have employed an assortment of mechanisms. The first attempt to power a pump with linearly contracting muscle was made in 1964 by Kusserow and Clapp who used a canine quadriceps femoris to actuate a levered extracorporeal pump (39). Since that time, several reports have been published describing various means to collect energy from linear muscle contractions, but relatively little emphasis has been placed on the detailed engineering needed to reduce these concepts to practice (40,41,42). As a result, these efforts have failed to produce a practical means by which contractile energy may be collected and transmitted in vivo to perform work within the body.

Current work focuses on eliminating the shortcomings of previous devices in order to produce a practical muscle energy converter (MEC) for long-term use. Recently, significant progress has been made by Trumble and Magovern with the manufacture of a prototype device designed to transform in situ muscle contractions into hydraulic power (43). This MEC, shown in Fig. 8, resembles a piston pump and is designed for implantation beneath the humeral insertion of the LD muscle. Viscous and inertial losses are minimized by transmitting hydraulic energy under conditions of high pressure and low flow. Short stroke lengths (1 cm) are employed to optimize device durability and minimize trauma to surrounding tissues. Preliminary in vitro testing has demonstrated >98% efficiency in converting input power to hydraulic energy and preload work. These results show that a significant amount of contractile energy can be efficiently transformed to hydraulic power via this mechanism.

Should MEC implant trials prove successful, this device could be coupled to a hydraulic blood pump to form a permanent muscle-actuated ventricular assist system (MAVAS) free of all external hardware. Such technology would provide a rel-

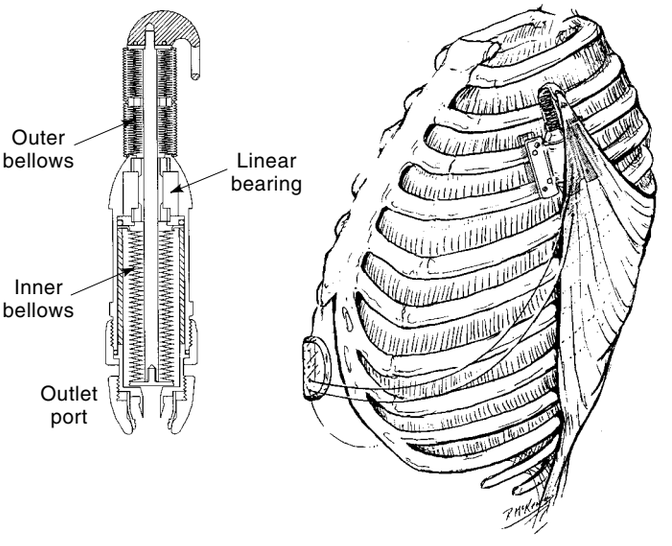


**Figure 8.** Left: Cross-sectional drawing of the MEC and its internal components (shown with the piston fully compressed). Right: Artist's conception of the MEC implanted beneath the latissimus dorsi muscle. The device is anchored to the ribcage via two titanium plates which fit into a groove machined into the cylindrical housing. Muscle contractions are controlled via an implanted stimulator (shown beneath the sternum) which delivers bursts of electrical impulses to the thoracodorsal nerve.

atively inexpensive alternative to heart transplantation and enable patients to retain a high quality of life. Alternate applications for such bio-actuated power supplies might also include driving respiratory support devices, providing sphincter control, and actuation of prosthetic limbs.

## OTHER ARTIFICIAL ORGANS

Implanted artificial organs have a wide range of energy and control requirements. Some need no external energy, for example prosthetic knees, hips, or cardiovascular stents. Others have modest energy needs which can be met for years by implanted batteries. These include the pacemaker and the cardioverter/defibrillator. The energy requirements for implanted cardiac pacemakers led to early designs for transcutaneously rechargeable systems, and spurred the development of lithium–iodine primary battery technology (44), the battery system still in general use today. Mechanical blood pumps, because of the substantial work they perform, cannot be powered for long with existing battery systems. Muscle-powered prostheses have the potential of providing high-energy output with only stimulus, command, and control functions, and these can be accommodated with implanted batteries. Implanted drug or insulin delivery systems are examples of fluid-pump artificial organs which do not require large amounts of energy to function.

### Functional Electrical Stimulation of Muscle

There are development efforts underway on systems intended to stimulate skeletal musculature to achieve postural maintenance (45) and even ambulation (46) for patients without voluntary muscle control, such as those with major damage to the spinal cord. In effect, the controller for these systems replaces an element of coordination normally performed by the spinal cord, brainstem, and cerebellum. One system undergoing clinical trials (47) provides hand grasp using electrodes implanted along and within the muscles of the forearm. Control is provided by shoulder muscle activation. These systems are designed to utilize the power available from the patients's own muscles. One limitation on these system designs is the restricted dynamic range in muscle force obtained from electrically stimulated muscle. The fine gradation of muscle force obtained by neural control is lost when stimulating muscle electrically, and rapid fatigue of muscles is the result. A second problem is the development of suitable artificial transducers for force and for position to control muscle-powered systems. The hope is that such designs for muscle stimulus may eventually be integrated with position and force information obtained from the physiological sensors to produce effective closed-loop controlled motion (48).

### Artificial Pancreas

Diabetes is a condition where the pancreas has lost its ability to regulate blood glucose levels through the release of insulin into the bloodstream. The resulting elevated blood-sugar levels have a number of serious consequences, including blindness, deficient wound-healing, and cardiovascular disease leading to early death. The lack of available organs and the need for antirejection drugs in pancreas recipients has limited the use of pancreas transplantation. As is the case with blood pumps, there are total artificial and hybrid approaches to the design of the artificial pancreas, and control system implementation is an important area of ongoing research.

Important hybrid systems undergoing development include the use of immunoisolated islets of Langerhans, the functional multicellular unit of the pancreas. These may be obtained either from human or from animal sources. These cells have the ability to naturally self-regulate insulin output in response to changes in blood sugar levels. Development efforts are directed at producing membranes which allow inward diffusion of glucose and oxygen and outward diffusion of insulin, while blocking elements of the immune system which would destroy the islets (49).

The total artificial approach to the artificial pancreas includes the clinically important externally worn infusion pump (eg, MiniMed 507, MiniMed, Fridley, Minnesota), in use by tens of thousands of patients. This device pumps insulin through a Teflon tube into the abdominal cavity at rates of up to about 1 $\mu$L/min. Worn externally it is readily refilled with insulin and batteries can be replaced as needed. Attempts to apply closed-loop control based on blood-glucose sensing have generally been unsuccessful. Sensor reliability remains a significant problem. Externally worn pumps run in an open-loop control configuration, with programmable basal rate, and elevated doses provided at mealtimes. A fully implantable intra-abdominal insulin pump is a long-term goal of continuing research efforts (50), and at least one design has been introduced for clinical use (Minimed MMT-2001, MiniMed, Fridley, Minnesota). This design eliminates the need for a percutaneous Teflon tube leading to the abdominal cavity. Periodic recharging of the insulin reservoir via hypodermic would be required. Lithium battery replacement would be needed at intervals of 3 years or more. In the case of the insulin pump, the flow rates are very low, and the pressure load within the abdomen is modest, so that the hydraulic workload is negligible. However, the electronics and pump energy requirements limit battery life. One advantage of the implanted insulin pump is that it may eventually provide a better location for stable glucose sensor operation and so enable fully closed-loop control for the artificial pancreas.

Support was received during the preparation of this section from NIH contracts N01-HV-38130 and N01-HV-58156 and by a grant from the Whitaker Foundation.

## BIBLIOGRAPHY

*Design and Control of Blood Pumps*

1. R. T. V. Kung et al., An atrial hydraulic shunt in a total artificial heart—A balance mechanism for the bronchial shunt, *Amer. Soc. Artif. Intern. Organs J.,* **39**: M213–M217, 1993.
2. A. J. Snyder et al., In vivo testing of a completely implanted total artificial heart system, *Amer. Soc. Artif. Intern. Organs J.,* **39**: M177–M184, 1993.
3. R. Rintoul et al., Continuing development of the Cleveland Clinic—Nimbus total artificial heart, *Amer. Soc. Artif. Intern. Organs J.,* **39**: M168–M171, 1993.
4. H. C. Kim et al., Development of a microcontroller-based automatic control system for the electrohydraulic total artificial heart, *IEEE Trans.,* Biomed. Eng. **44**: 77–89, 1997.

5. H. Konishi et al., Long-term animal survival with an implantable axial flow pump as a left ventricular assist device, *Artif. Organs,* **20** (2): 124–127, 1996.
6. R. J. Kaplon et al., Miniature axial flow pump for ventricular assistance in children and small adults, *J. Thorac. Cardiovasc. Surg.,* **111** (1): 13–18, 1996.
7. L. A. R. Golding and W. A. Smith, Cleveland Clinic rotodynamic pump, *Ann. Thorac. Surg.,* **61**: 457–462, 1996.
8. K. Kawahito et al., *Ex vivo* evaluation of the NASA/DeBakey axial flow ventricular assist device, *Amer. Soc. Artif. Intern. Organs J.,* **42** (5): M754–757, 1996.
9. A. J. Snyder, G. Rosenberg, and W. S. Pierce, Noninvasive control of cardiac output for alternately ejecting dual-pusherplate pumps, *Artif. Organs,* **16**: 182–194, 1992.
10. A. J. Snyder, G. Rosenberg, and D. L. Landis, Indirect estimation of circulatory pressures for control of an electric motor driven total artificial heart, *Adv. Bioeng.,* 87–88, 1985.
11. J. F. Gardner et al., Aortic pressure estimation with electro-mechanical circulatory assist devices, *J. Biomech. Eng.,* **115**: 187–194, 1993.
12. D. B. Geselowitz, G. E. Miller, and W. M. Phillips, Dynamic mode of a c-type pneumatically driven artificial ventricle, *J. Biomech. Eng.,* 14–19, 1977.
13. T. Kitamura, T. Kijima, and H. Akashi, Modeling technique of prosthetic heart valves, *J. Biomech. Eng.,* **106**: 83–88, 1984.
14. G. Rosenberg et al., Design of and evaluation of the Penn State mock circulatory system, *Am. Soc. Artif. Organs J.,* **4**: 41–49, 1981.
15. N. C. Kelley et al., Noninvasive control of the Penn State total artificial heart: A computer simulation, *Proc. Northeast Bioeng. Conf.,* 22–23, March 1995.
16. L. Martin et al., Non-invasive control of aortic pressure and cardiac output in a reciprocating pusher-plate artificial heart, *Proc. Northeast Bioeng. Conf.,* pp. 62–63, March 1996.
17. G. Rosenberg et al., Power requirements for an electric motor-driven total artificial heart, *Proc. IEEE 9th Annu. Conf. Eng. Med. Biol. Soc.,* 1987, pp. 188–189.
18. B. P. Griffith et al., Results of extended bridge to transplantation: Window into the future of permanent ventricular assist devices, *Ann. Thorac. Surg.,* **61**: 396–398, 1996.

*Transcutaneous Energy Transmission*

19. F. C. Flack, E. D. James, and C. M. Schlapp, Mutual inductance of air-cored coils: Effect on design of radio-frequency coupled implants. *Med. Biol. Eng.,* **9**: 79–85, 1971.
20. M. Soma, D. Galbraith, and R. L. White, Radio-frequency coils in implantable devices: Misalignment analysis and design procedure, *IEEE Trans. Biomed. Eng.,* **34**: 276–282, 1987.
21. F. E. Terman, *Radio Engineering,* 2nd ed., New York: McGraw-Hill, 1937.
22. D. B. Geselowitz, Q. T. N. Hoang, and R. P. Gaumond, The effects of metals on a transcutaneous energy transmission system, *IEEE Trans. Biomed. Eng.,* **39**: 928–934, 1992.
23. C. Sherman et al., Research and development: Systems for transmitting energy through intact skin, *Final Technical Report N01-HV-0-2903-3,* Thermo Electron Corp., Waltham, MA, July 1983.
24. W. J. Weiss et al., In vivo performance of a transcutaneous energy transmission system with the Penn State motor driven ventricular assist device, *Trans. Am. Soc. Artif. Intern. Organs,* **35** (3): 284–288, 1989.
25. J. S. Brugler et al., Transcutaneous power transmission and electronic control of a ventricular assist system, *Proc. IEEE 8th Annu. Conf. Eng. Med. Biol. Soc.,* 73–76, 1986.
26. J. C. Schuder, J. H. Gold, and H. E. Stephenson, Jr., An inductively coupled rf system for the transmission of 1 kW of power through the skin, *IEEE Trans. Biomed. Eng.,* **BME-18**: 265–273, 1971.
27. D. C. Galbraith, M. Soma, and R. L. White, A wide-band efficient inductive transdermal power and data link with coupling insensitive gain, *IEEE Trans. Biomed. Eng.,* **34**: 265–275, 1987.
28. J. A. Miller, G. Belanger, and T. Mussivand, Development of an autotuned transcutaneous energy transfer system, *Amer. Soc. Artif. Intern. Organs, J.,* **39** (3): M706–M710, 1993.

*Muscle-Powered Blood Pumps*

29. S. Salmons and F. Sreter, Significance of impulse activity in the transformation of skeletal muscle type, *Nature,* **263**: 30–34, 1976.
30. D. R. Trumble and J. A. Magovern, Ergometric studies of untrained skeletal muscle demonstrate feasibility of muscle-powered cardiac assistance, *J. Appl. Physiol.,* **77** (4): 2036–2041, 1994.
31. F. Ugolini, Skeletal muscle for artificial heart drive: Theory and in vivo experiments. In: *Biomechanical Cardiac Assist: Cardiomyoplasty and Muscle-Powered Devices,* Mount Kisko, NY: Futura, 1986, pp. 193–210.
32. S. Salmons and J. C. Jarvis, The working capacity of skeletal muscle transformed for use in a cardiac assist role. In: *Transformed Muscle for Cardiac Assist and Repair,* Mount Kisko, NY: Futura, 1990, pp. 89–104.
33. J. C. Jarvis, Power production and working capacity of rabbit tibialis anterior muscles after chronic electrical stimulation at 10 Hz, *J. Physiol.* (*Great Britain* ) **470**: 157–169, 1993.
34. S. Salmons and J. C. Jarvis, Cardiac assistance from skeletal muscle: A critical appraisal of the various approaches, *Br. Heart J.,* **68**: 333–338, 1992.
35. W. N. Stainsby and G. M. Andrew, Maximal blood flow and power output of dog muscle in situ, *Med. Sci. Sports Exercise,* **20**: S109–S112, 1988.
36. C. A. Doorn et al., Latissimus dorsi muscle flow during synchronized contraction: Implications for cardiomyoplasty, *Ann. Thor. Surg.,* **61**: 603–609, 1996.
37. N. W. Guldner et al., Dynamic training of skeletal muscle ventricles: A method to increase muscular power for cardiac assistance, *Circulation,* **89**: 1032–1040, 1994.
38. R. L. Whalen et al., A skeletal muscle powered ventricular assist device (BAD), *Amer. Soc. Artif. Intern. Organs, J. Abstracts,* **42** (2): 132, 1996.
39. B. Kusserow and J. Clapp, A small ventricle-like pump for prolonged perfusions: Construction and initial studies, including attempts to power a pump biologically with skeletal muscle, *Trans. Amer. Soc. Artif. Intern. Organs,* **10**: 74–78, 1964.
40. D. Spitzer, An implantable power source for an artificial heart or left ventricular assist device, *Trans. Amer. Soc. Artif. Intern. Organs,* **31**: 193–195, 1985.
41. D. J. Farrar and J. D. Hill, A new skeletal linear-pull energy convertor as a power source for prosthetic circulatory support devices, *J. Heart Lung Transplant,* **11**: S341–S350, 1992.
42. M. Takahashi et al., Efficacy of a skeletal muscle-powered dynamic patch: Part 1. Left ventricular assistance, *Ann. Thor. Surg.,* **59**: 305–312, 1995.
43. D. R. Trumble and J. A. Magovern, A permanent prosthesis for converting in situ muscle contractions into hydraulic power for cardiac assist, *J. Appl. Physiol.,* **82** (5): 1704–1711, 1997.

*Other Artificial Organs*

44. W. Greatbach et al., The solid state lithium battery, *IEEE Trans. Biomed. Eng.,* **BME-18**: 317, 1971.
45. N. de N. Donaldson and C.-H. Yu, FES standing: Control by handle reactions of leg muscle stimulation (CHRELMS), *IEEE Trans. Rehabil. Eng.,* **4**: 280–287, 1997.
46. D. A. Winter, *Biomechanics and Motor Control of Human Movement,* New York: Wiley Interscience, 1990.
47. K. S. Wuolle et al., Development of a quantitative hand grasp and release test for patients with tetraplegia using a hand neuroprosthesis, *J. Hand Surgery,* **19A**: 209–218, 1994.
48. T. R. D. Scott, P. H. Peckham, and K. L. Kilgore, Tri-state myoelectric control of bilateral upper extremity neuroprostheses for tetrapleic individuals, *IEEE Trans. Rehabil. Eng.,* **4**: 251–263, 1997.
49. C. K. Colton and E. S. Avgoustiniatos, Bioengineering in development of the hybrid artificial pancreas, *Trans. ASME (Biomechanics),* **113**: 152–170, 1991.
50. T. Buchwald, D. Rhode, and K. Kernstine, Insulin delivery by implanted pump: A chronic treatment for diabetes, *Trans. Am. Soc. Artif. Intern. Organs,* **35**: 5–7, 1989.

ROGER P. GAUMOND
JOHN F. GARDNER
ALAN J. SNYDER
WILLIAM J. WEISS
Penn State University
CHRISTOPHER KELLEY
Boston University School of Medicine
DENNIS R. TRUMBLE
Allegheny University of the Health Sciences (Allegheny Campus)